Physical Review & Research International
3(4): 674-687, 2013

SCIENCEDOMAIN *international*
www.sciencedomain.org

Microstructure of Self-Consolidating High Strength Concrete Incorporating Palm Oil Fuel Ash

M. A. Salam[1], Md. Safiuddin[1*] and M. Z. Jumaat[1]

[1]Department of Civil Engineering, Faculty of Engineering, University of Malaya, 50603 Kuala Lumpur, Malaysia.

Authors' contributions

The work presented in this paper was carried out in collaboration between all authors. Author MAS performed the experimental research taking guidance from authors MS and MZJ. The primary manuscript of the paper was prepared by author MAS but reviewed and corrected by author MS. All authors reviewed and approved the final manuscript.

Research Article

Received 16th May 2013
Accepted 25th June 2013
Published 3rd August 2013

ABSTRACT

This paper mainly focuses the effect of palm oil fuel ash (POFA) on the microstructure of self-consolidating high-strength concrete (SCHSC). POFA has been used as a supplementary cementing material replacing ordinary portland cement (OPC) in the range of 0-30%. SCHSC mixes were produced with the water-to-binder (W/B) ratios of 0.25-0.40 to obtain high strength. The microstructure of 28 and 56 days old concretes was analyzed based on their scanning electron micrographs (SEMs) in the cases of 0 and 20% POFA contents. The influence of POFA on the 28 and 56 days compressive strength and permeable porosity was also investigated. The experimental results showed that a POFA content up to 20% increases the compressive strength of SCHSC compared with that of the control concrete due to the reduced permeable porosity. The SEMs of the concretes revealed that POFA contributes to producing a denser microstructure, which increases the compressive strength and reduces the permeable porosity of SCHSC.

Keywords: Compressive strength; concrete microstructure; palm oil fuel ash; permeable porosity; scanning electron micrograph; self-consolidating high-strength concrete.

[*]Corresponding author: Email: safiq@yahoo.com, msafiudd@uwaterloo.ca;

1. INTRODUCTION

The silica (S_iO_2) content of the ash obtained as industrial by-product or agro-waste is an important factor for its usefulness in the production of concrete. When ash is added to cement, the silica participates in pozzolanic reaction to form additional calcium silicate hydrate (C-S-H) in the hydrated cement matrix, increases the density of the matrix, and refines the pore structure [1,2]. The additional C-S-H produced makes the microstructure of concrete denser and improves the interfacial bond between aggregates and binder paste, thus improving the strength, transport properties and durability of concrete [3]. Some ashes such as fly ash, rice husk ash, and bagasse ash possess a considerable amount of silica content, which acts to enhance the hardened properties of concrete [1-4]. Similarly, palm oil fuel ash (POFA) contains a significant amount of S_iO_2, which may contribute to producing a denser microstructure in concrete.

POFA is a waste material produced after the extraction of oil from the fresh fruit bunches of oil palm tree. This ash is mostly dumped in open field near palm oil mills without any profitable return, thus causing environmental pollution and health hazard [5,6]. It has been found that the properly processed POFA can be used successfully as a supplementary cementing material (SCM) for producing various types of concrete [7]. The use of POFA in concrete contributes to enhance the quality of concrete with respect to strength and durability due to its micro-filling ability and pozzolanic property [8,9]. In the pozzolanic reaction, the SiO_2 and Al_2O_3 contents of POFA involve in the reaction with $Ca(OH)_2$ to form C-S-H and calcium aluminate hydrate (C-A-H). The Al_2O_3-SiO_2 framework can also be formed from pozzolanic reaction. However, the main reaction product of pozzolanic reaction is C-S-H gel that enhances the strength of cement paste as well as improves the microstructure of concrete [10].

Several researchers have studied the microstructural aspects of concrete using various types of ashes. Zhang et al. [2] investigated the microstructure of concrete incorporating rice husk ash and observed a higher compressive strength for this concrete compared with the control concrete due to the reduced porosity, reduced $Ca(OH)_2$ (portlandite), and reduced width of interfacial transition zone between aggregate and cement paste. The morphology of hydrates in concrete containing ground granulated blast-furnace slag have been studied by Gao et al. [11]; they observed that the weak interfacial transition zone between aggregate and cement paste was strengthened as a result of the pozzolanic reaction of slag. Tuan et al. [12] carried out the microstructural analyses of ultra high-performance concretes incorporating rice husk ash and silica fume at 28 days; they found that the addition of rice husk ash can increase the degree of cement hydration at later ages; they also observed that the thickness of the interfacial transition zone between sand particles and cement matrix (cement plus rice husk ash or cement plus silica fume) was very small at the age of 28 days. Altwair et al. [13] investigated the microstructural effect of treated POFA at 90 days of curing; They found that the amount of $Ca(OH)_2$ liberated from cement hydration gradually decreased with an increased POFA content and the C-S-H compound was identified as the main product of the reaction between POFA and $Ca(OH)_2$. The results of SEM analysis confirmed that there was an increased degree of pozzolanic reaction when the POFA-to-cement ratio was up to 0.30. Eldagal [14] investigated the microstructure of high strength concrete (HSC) including POFA at 3 and 7 days of curing based on the SEM analysis; the porous morphology was observed in POFA concrete at 3 days; the fine needle like structures of ettringite crystals were observed at 7 days, some hexagonal platelets of $Ca(OH)_2$ was also observed in several samples that had relatively a lower strength at 7 days.

However, limited studies have been carried out to examine the microstructure of SCHSC at the optimum POFA content providing the highest compressive strength and lowest porosity.

This paper presents an experimental study on the effects of POFA on the compressive strength and permeable porosity of SCHSC. The optimum POFA content was determined based on the results of compressive strength and permeable porosity. Above all, the effect of optimum POFA content on the microstructure of SCHSC has been highlighted in this study. In addition, this study discusses how the compressive strength and permeable porosity of SCHSC were influenced by its microstructure.

2. MATERIALS AND METHODOLOGY

2.1 Materials

The coarse aggregate (CA) used in this study was crushed granite stone whereas the fine aggregate (FA) used was the mining sand. The ordinary (ASTM Type I) portland cement (OPC) was used as the main cementing material. POFA was used as a supplementary cementing material substituting 0–30% of OPC. POFA and OPC together acted as the binder (B). The mixing water (W) used was normal tap water. A polycarboxylate based high-range water reducer (HRWR) was also used in the present study to achieve the self-consolidation capacity of concrete. Both CA and FA were tested to determine their specific gravity, water absorption, bulk density, moisture content, and gradation. The sieve analyses of CA and FA were conducted according to ASTM C 136-06 [15] to examine their gradation. The POFA obtained at 800–1000ºC was processed through proper grinding to increase its fineness greater than that of cement. POFA and OPC were tested for their specific gravity, particle size distribution, sieve fineness, and specific surface area. The HRWR was tested for its specific gravity and solid content. The physical properties CA, FA, OPC, POFA and HRWR are given in Table 1. The gradation of CA and FA are shown in Tables 2 and 3, respectively. The particle characteristics of POFA and OPC were examined by a scanning electron microscope. The unground POFA particles were large, mostly spherical, and more porous whereas the particles of ground POFA were small, mostly angular, and less porous, as can be seen from Fig. 1.

Table 1. Physical properties of constituent materials

Properties	CA	FA	OPC	POFA	HRWR
Specific gravity	2.62	2.69	3.16	2.48	1.05
Median particle size, d_{50} (μm)	-	-	14.6	9.5	-
% Mass passing through 45-μm sieve	-	-	91.5	95	-
Specific surface area, Blaine (m^2/kg)	-	-	351	775	-
Specific surface area, BET (m^2/kg)	-	-	3046	4103	-
Pozzolanic activity index (28 days) (%)	-	-	-	105	-
Solid content (%)	-	-	-	-	30
Absorption capacity (%)	0.55	1.32	-	-	-
Moisture content (%)	0.27	0.31	-	-	-
Fineness modulus	6.76	2.88	-	-	-
Bulk density (oven-dry) (kg/m^3)	1513	1700	-	-	-
Co-efficient of gradation	1.11	1.05	-	-	-

Table 2. Gradation of coarse aggregate

Sieve size (mm)	Weight retained (gm)	% retained	Cumulative % retained	% finer	ASTM limit (% finer)	Fineness modulus
75.0	0.0	0.00	0.00	100.0	100	6.76
37.5	0.0	0.00	0.00	100.0	100	
19.0	65.4	3.2	3.2	96.8	90-100	
9.5	1424.3	71.2	74.4	25.6	20-55	
4.75	483.7	24.2	98.6	1.4	0-10	
2.36	26.6	1.3	100.0	0.0	-	
1.18	-	0.00	100.0	0.0	-	
0.6	-	0.00	100.0	0.0	-	
0.3	-	0.00	100.0	0.0	-	
0.15	-	0.00	100.0	0.0	-	
Pan	-	-	-	-	-	
Total	2000.0	-	676.2	-	-	

Table 3. Gradation of fine aggregate

Sieve size (mm)	Weight retained (gm)	% retained	Cumulative % retained	% finer	ASTM limit (% finer)	Fineness modulus
4.75	23.5	4.7	4.7	95.3	95-100	2.88
2.36	59.5	11.9	16.6	83.4	80-100	
1.18	92.5	18.5	35.1	64.9	50-85	
0.6	108.5	21.7	56.8	43.2	25-60	
0.3	115.5	23.1	79.9	20.1	10-30	
0.15	75.0	15.0	94.9	5.1	0-10	
Pan	25.5	-	-	-	-	
Total	500.0	-	288.0	-	-	

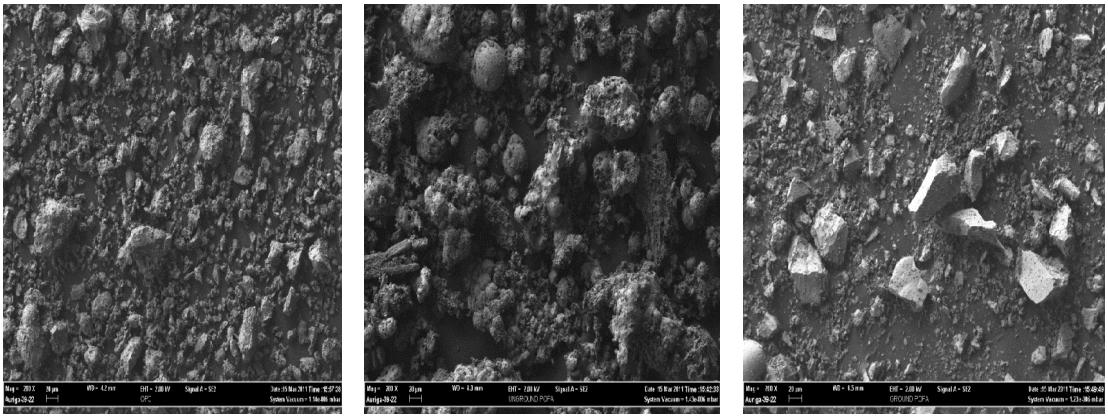

(a) (b) (c)

Fig. 1. Scanning electron micrograph (SEM) of (a) OPC, (b) unground POFA, and (c) ground POFA

2.2 Mix Proportions of Concrete

In total, twenty SCHSC mixes were prepared with different water-to-binder (W/B) ratios and POFA contents. OPC was partially replaced by 0%, 10%, 20%, 25%, and 30% POFA by weight. The W/B ratios of 0.25, 0.30, 0.35, and 0.40 were used to produce high strength. The amount of mix water was selected based on the guideline given in ACI 211.4R-08 [16] whereas the amount of cement was calculated based on the selected W/B ratios. The optimum fine aggregate/total aggregate (FA/TA) ratio was determined based on the maximum bulk density of aggregate blends and it was 0.50 for all SCHSC mixes. The HRWR dosages were fixed to ensure that the concretes had self-consolidation capacity (slump flow in the range of 600–800 mm; the HRWR dosage to achieve this slump flow varied due to different W/B ratios and POFA contents). The detailed mix proportions for various SCHSC mixes are given in Table 4. The SCHSC mixes were designated based on their W/B ratio and POFA content. For example, C25P0 implies an SCHSC mix whose W/B ratio and POFA content is 0.25 and 0%, respectively.

Table 4. Mix proportions of different concrete mixes

Concrete type	W/B ratio	CA (kg/m^3)	FA (kg/m^3)	OPC (kg/m^3)	POFA (% B)	(kg/m^3)	W (kg/m^3)	HRWR (% B)
C25P0	0.25	780.0	779.7	705.9	0	0	176.5	1.8
C25P10	0.25	772.0	771.4	635.3	10	70.6	176.5	1.845
C25P20	0.25	763.0	761.0	564.7	20	141.2	176.5	1.875
C25P25	0.25	758.0	757.9	529.4	25	176.5	176.5	2
C25P30	0.25	754.0	752.1	494.1	30	211.8	176.5	2.1
C30P0	0.30	834.0	833.2	588.2	0	0	176.5	1.5
C30P10	0.30	827.0	825.6	529.4	10	58.8	176.5	1.575
C30P20	0.30	819.0	817.1	470.6	20	117.6	176.5	1.8
C30P25	0.30	815.0	813.3	441.2	25	147.1	176.5	1.875
C30P30	0.30	811.0	809.9	411.8	30	176.5	176.5	1.925
C35P0	0.35	872.0	871.4	504.2	0	0	176.5	1.2
C35P10	0.35	867.0	865.3	453.8	10	50.4	176.5	1.225
C35P20	0.35	860.0	858.5	403.4	20	100.8	176.5	1.25
C35P25	0.35	856.0	855.5	378.2	25	126.1	176.5	1.5
C35P30	0.35	853.0	851.9	352.9	30	153.3	176.5	1.575
C40P0	0.40	901.0	899.5	441.2	0	0	176.5	1.0
C40P10	0.40	895.0	894.9	397.1	10	44.1	176.5	1.05
C40P20	0.40	890.0	888.2	352.9	20	88.2	176.5	1.2
C40P25	0.40	887.0	885.9	330.9	25	110.3	176.5	1.225
C40P30	0.40	884.0	882.1	308.8	30	132.4	176.5	1.4

2.3 Preparation and Testing of Concretes

The fresh concretes were prepared according to the procedure described in Safiuddin [3].The concrete was produced with a self-consolidation capacity. Immediately after the completion of mixing, the slump flow of the fresh concretes was determined to examine their self-consolidation capacity. The slump flow was determined according to ASTM C 1611/C 1611M-09a [17].

The cylinder moulds of Ø100×200 mm were cast for the compressive strength and porosity tests of concrete. Upon completion of casting, the specimens were left undisturbed and covered with plastic sheet and wet burlap to avoid evaporation. The specimens were de-moulded, marked, and transferred to the curing tank for wet curing at the age of 24 ± 4 h. The curing temperature was 23 ± 2^0C. The wet curing was continued until the day of testing. The compressive strength was determined at 28 and 56 days by testing triplicate Ø100×200 mm cylinder specimens according to ASTM C 39/ C 39M [18]. The permeable porosity was determined at 28 and 56 days by testing triplicate Ø100×50 mm cylinder specimens according to ASTM C 642 [19]. These specimens were obtained by cutting Ø100×200 mm cylinder specimens.

The effect of POFA on the microstructure of SCHSC was examined by analyzing the scanning electron micrograph (SEM) of several concretes with and without POFA. The C25P0, C25P20, C30P0, C30P20, C35P0, C35P20, C40P0, and C40P20 concretes after 28 and 56 days of curing were mainly considered for microstructural analysis. In addition, the microstructure of C35P0 and C35P20 concretes was tested at the ages of 3 and 7 days to observe the effect of POFA at the early stage of concrete. It should be mentioned that all POFA concretes contained the optimum amount of POFA (20%), which was obtained from the results of compressive strength and permeable of porosity. For the SEM analyses, the concretes were crushed at 3, 7, 28, and 56 days of curing as per the selected testing ages; the SEM samples were collected from the crushed concrete and then put in a glass container with acetone to hold further hydration until the day of testing. This was followed by drying the SEM samples in a vacuum oven at 105ºC for approximately two hours before testing. Twenty pictures were collected; ten were without POFA and the rest were with 20% POFA. The magnification for the microstructural analysis of 3, 7, 28 days and 56 days concretes was 2,000 to 20,000 times to get the suitable images. In the cases of the early-age concretes, the magnification for C35P0 and C35P20 was 2,000 and 20,000 times, respectively. The SEM images were taken using a Zeiss Auriga FIB-SEM machine. The electron high tension (EHT) value for the tests was 2 kV throughout the study. Generally, the EHT value ranges from 200V to 30 kV. The EHT used in the present study was sufficient to provide good image. Furthermore, the working distance (WD), which is the distance between the sample surface and the lower portion of the lens, should be greater than 4 mm. The WD was 4.1 to 9.1 mm in the present study.

3. RESULTS AND DISCUSSION

3.1 Self-Consolidation Capacity of Concretes

The self-consolidation capacity of SCHSC is generally measured with respect to slump flow. The slump flow of SCHSC must be ≥ 600 mm to achieve self-consolidation capacity. In this study, the slump flow varied in the range of 605–720 mm as shown in Table 5. The slump flow results revealed that the concretes had the self-consolidating capacity as they provided a slump flow greater than 600 mm [20]. Adequate HRWR dosage was used to obtain the self-consolidation capacity of concrete. HRWR dispersed the cement particles by its steric hindrance effect induced by long grafted side-chain, and thus reduced the loss of free water due to entrapping in cement flocks [21]. As a result, more free water was available to achieve self-consolidation capacity.

3.2 Compressive Strength of Concretes

The compressive strength of the concretes at each testing age was the average of the strength values obtained from three Ø100×200 mm cylinder specimens. The average compressive strength of SCHSCs at 28 and 56 days are shown in Table 5. The 28 days compressive strength varied from 52.3 to 74.2 MPa while the 56 days compressive strength differed from 54.8 to 77.0 MPa for different SCHSCs.

The POFA content influenced the compressive strength of concrete. It is obvious from Table 5 that the compressive strength of concretes increased with the increase in POFA content up to a certain level. The maximum strength gain occurred at the replacement level of 20%. Beyond this replacement level, a gradual reduction in compressive strength was observed. The compressive strength of POFA concretes increased due to the pozzolanic behaviour of POFA. This can be supported based on the strength activity index of POFA. In the present study, the strength activity index of POFA was 105% (Table 1); it is higher than the minimum limit of 75% for pozzolanic supplementary cementing materials, as specified in ASTM C 618-08a [22]. The high SiO_2 content (62.3%) of the ground POFA reacted with $Ca(OH)_2$ (liberated from cement hydration) to produce an additional calcium silicate hydrate (C-S-H), which improved the compressive strength of concrete. Furthermore, POFA had a higher surface area due to smaller particles, and therefore enhanced the pozzolanic activity and hence the compressive strength of concrete [23]. The micro-filling ability of POFA also contributed to increase the compressive strength of SCHSC. The average particle size of POFA was lower than that of OPC. Therefore, the finer POFA particles filled in the micro-voids in cement paste, thus improving the microstructure of concrete to produce a higher compressive strength.

Table 5. Fresh and hardened properties of different concretes

Concrete type	Slump flow (mm)	Compressive strength (MPa)		Permeable porosity (%)	
		28 days	56 days	28 days	56 days
C25P0	660	70.9	72.9	7.98	7.58
C25P10	680	72.9	75.5	7.51	7.18
C25P20	705	74.2	77.0	7.04	6.88
C25P25	710	68.2	70.8	7.97	7.60
C25P30	720	65.9	68.4	8.10	7.71
C30P0	640	67.6	69.5	8.95	8.60
C30P10	655	69.3	72.1	8.59	8.30
C30P20	670	71.3	74.1	8.21	8.10
C30P25	680	65.5	68.1	8.97	8.62
C30P30	700	63.1	65.6	9.12	8.71
C35P0	630	61.4	63.2	9.99	9.85
C35P10	640	62.8	65.5	9.70	9.42
C35P20	665	64.2	66.9	9.43	8.93
C35P25	670	58.8	61.6	9.93	9.85
C35P30	675	57.7	60.3	10.25	10.13
C40P0	605	56.2	58.0	11.16	10.96
C40P10	620	57.9	60.2	10.92	10.59
C40P20	630	58.2	60.8	10.59	10.39
C40P25	635	54.1	56.8	11.20	11.10
C40P30	645	52.3	54.8	11.50	11.25

3.3 Permeable Porosity of Concretes

The average test results for the 28 and 56 days permeable porosity of SCHSCs obtained by testing three Ø100×50 mm cylinder specimens are shown in Table 5. The permeable porosity varied in the range of 7.04 to 11.50% at 28 days whereas 6.88 to 11.25% at 56 days. The lowest level of permeable porosity was obtained for the concrete with 20% POFA content. The overall test results of the permeable porosity suggest that the quality of the concretes was good. According to Hearn et al. [24] the permeable porosity of high-quality concrete is 7% whereas that of the average-quality concrete is 15%.

The POFA content influenced the permeable porosity of concrete. In the present study, the permeable porosity of concrete decreased for 10 and 20% POFA contents but increased for 25 and 30% POFA contents, as evident from Table 5. The amount of silica (SiO_2) available at 20% POFA content was probably utilized completely to produce the maximum amount of additional or secondary C-S-H. Hence, the optimum POFA content was 20%, which produced the minimum permeable porosity by filling in the micro-voids in cement paste with additional C-S-H.

3.4 Microstructure of Concretes

Scanning electron microscopy was used to study the microstructure of concretes. The concretes with 0 and 20% POFA (optimum POFA content) were selected to observe the microstructure. This is because 20% POFA produced the highest level of compressive strength and the lowest level of permeable porosity at 28 and 56 days, thus indicating an optimum level of improvement in microstructure.

POFA improved the microstructure of concrete at both early and later ages. Figs. 2 and 3 show the SEM images of C35P0 and C35P20 to present a comparison between the microstructures of SCHSCs with and without POFA at the early ages of 3 and 7 days. Both C35P0 and C35P20 were more porous at 3 days than at 7 days, as obvious from Figs. 2 and 3. However, the concrete microstructure was relatively less porous in the presence of 20% POFA. The fine needle-like ettringites were observed in C35P0 at the ages of 3 and 7 days. Some ettringites were observed in C35P20 at the age of 3 days; however, they disappeared at the age of 7 days, as evident from Fig. 3(b). Moreover, substantial hexagonal platelets of $Ca(OH)_2$ were observed in C35P0 at the ages of 3 and 7 days, as obvious from Figs. 2(a) and 3(a). These $Ca(OH)_2$ crystals were significantly reduced in C35P20 incorporating 20% POFA, as can be seen from Figs. 2(b) and 3(b). As a result, the concrete (C35P20) became less porous. Similar observations were made by Eldagal [14] in the case of POFA concrete.

The microstructure of SCHSCs changed with the curing age of concrete. Figs. 4 to 7 show the SEM images of the 28 and 56 days old concretes (C25P0, C25P20; C30P0, C30P20; C35P0, C35P20; C40P0, C40P20) to present a comparison between the microstructures of later-age SCHSCs with and without POFA. The C-S-H was the predominant product phase at both ages (28 and 56 days) for all concretes. There was no needle-like ettringite product in the SEM of all concretes. The ettringite is generally formed at the early ages (≤ 7 days) of hydration and disappeared as the cement hydration continues beyond 7 days. Some $Ca(OH)_2$ crystals were seen in the SEMs of the concretes without POFA (refer to the SEMs of C25P0, C30P0, C35P0, and C40P0 in Figs. 4 to 7). These crystals were significantly reduced in all concretes including 20% POFA (refer to the SEMs of C25P20, C30P20, C35P20, and C40P20 in Figs. 4 to 7). This is attributed to the pozzolanic activity of POFA

that produced additional C-S-H at 28 and 56 days. The $Ca(OH)_2$ crystals were consumed when reacted with the silica (SiO_2) content of POFA through pozzolanic reaction. A similar effect was observed by Gao et al. [11] in the case of ground granulated blast-furnace slag.

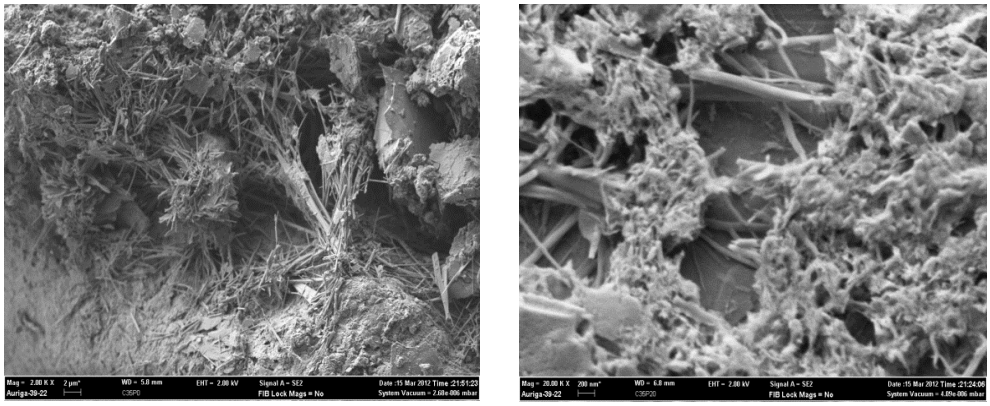

(a) C35P0 (3 days) (b) C35P20 (3 days)

Fig. 2. Effect of POFA on the microstructure of concrete (W/B = 0.35; 3 days)

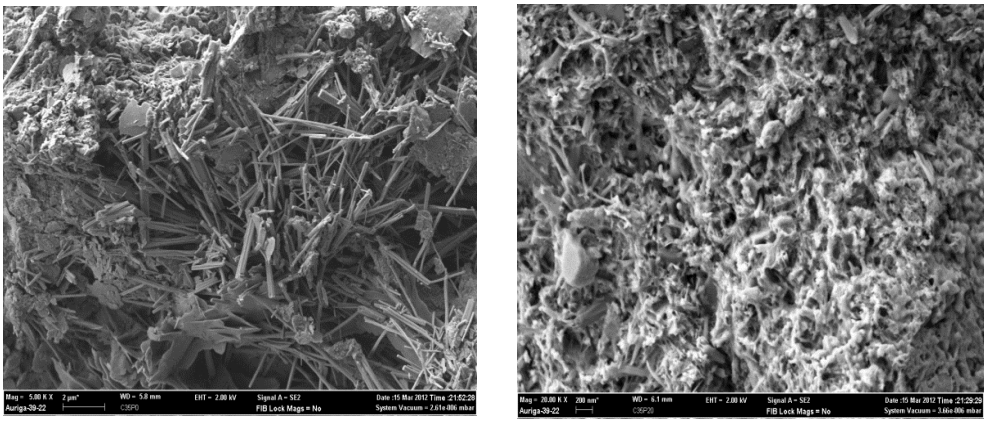

(a) C35P0 (7 days) (b) C35P20 (7 days)

Fig. 3. Effect of POFA on the microstructure of concrete (W/B = 0.35; 7 days)

The POFA concretes were less porous than the non-POFA concretes, as understood from the SEMs presented in Figs. 4 to 7. This suggests that POFA contributed to produce a denser microstructure in SCHSC at both ages due to its microfilling ability and pozzolanic activity. The improvement of concrete microstructure occurred in both bulk paste matrix and interfacial transition zone (the zone between aggregate and bulk cement or binder paste matrix) with a reduced porosity, as evident from the SEM images of the concretes with and without POFA. In particular, the porosity and width of interfacial transition zone were substantially reduced in the presence of 20% POFA, as can be realized from Figs. 4(a) and 4(b). As a result, the compressive strength increased and the permeable porosity decreased for the SCHSCs with 20% POFA content. Zhang et al. [2] observed a similar effect in the case of high-strength concrete including rice husk ash.

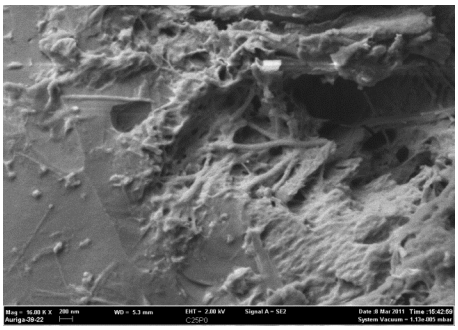

(a) C25P0 (28 days)

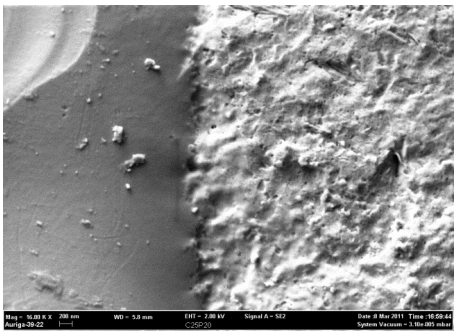

(b) C25P20 (28 days)

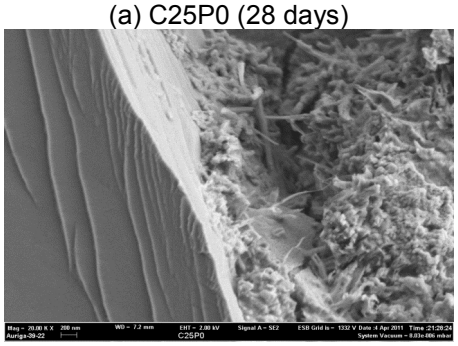

(c) C25P0 (56 days)

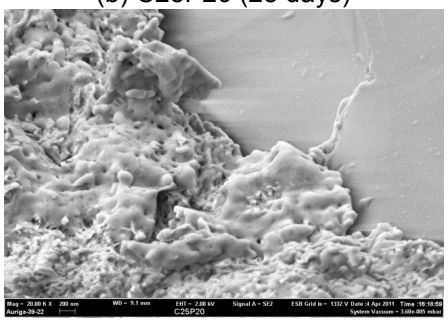

(d) C25P20 (56 days)

Fig. 4. Effect of POFA on the microstructure of concrete (W/B = 0.25; 28 and 56 days)

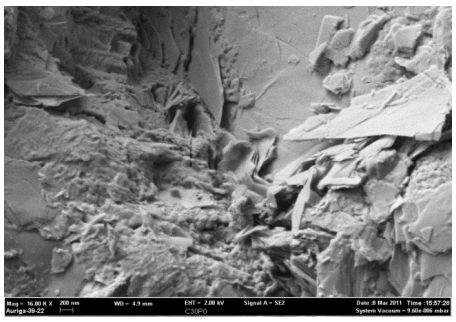

(a) C30P0 (28 days)

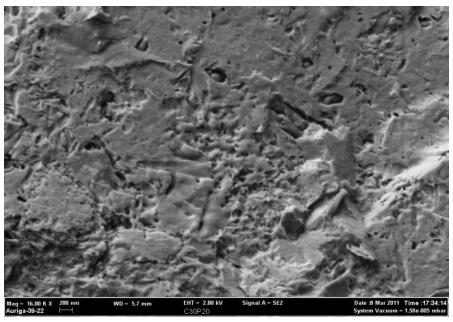

(b) C30P20 (28 days)

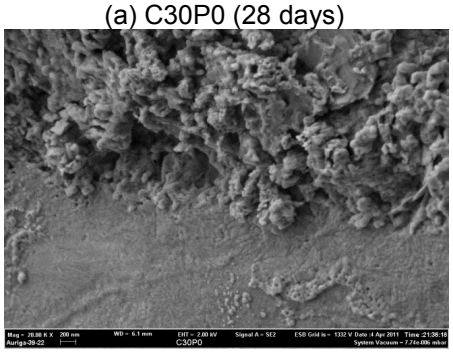

(c) C30P0 (56 days)

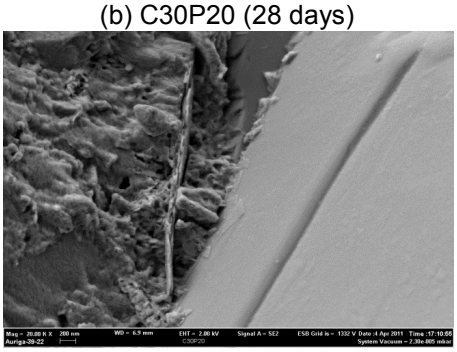

(d) C30P20 (56 days)

Fig. 5. Effect of POFA on the microstructure of concrete (W/B = 0.30; 28 and 56 days)

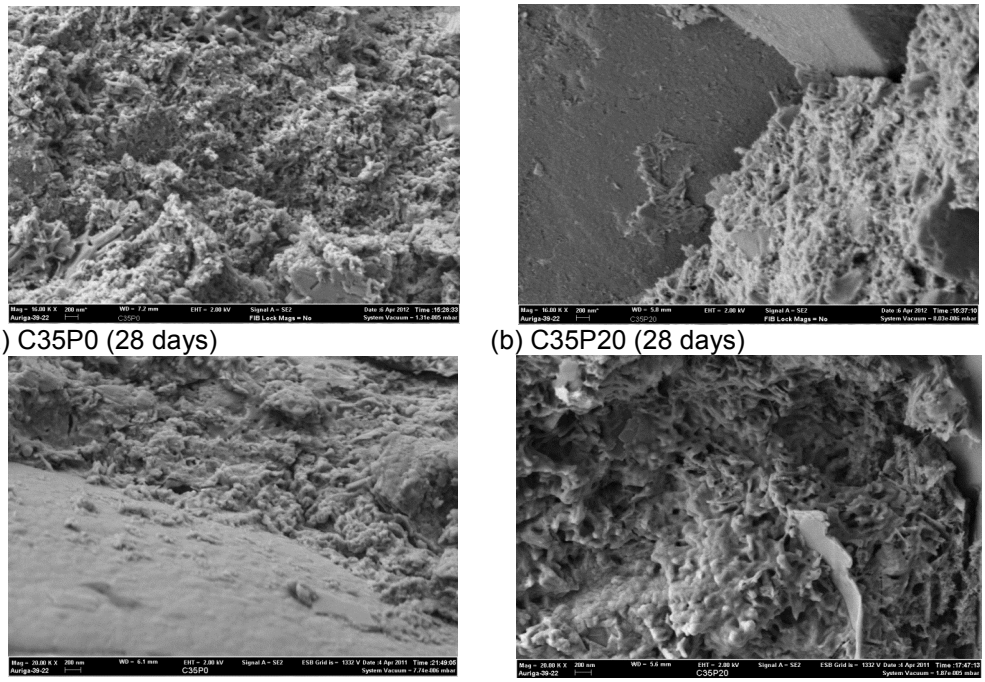

(a) C35P0 (28 days) (b) C35P20 (28 days)

(c) C35P0 (56 days) (d) C35P20 (56 days)

Fig. 6. Effect of POFA on the microstructure of concrete (W/B = 0.35; 28 and 56 days)

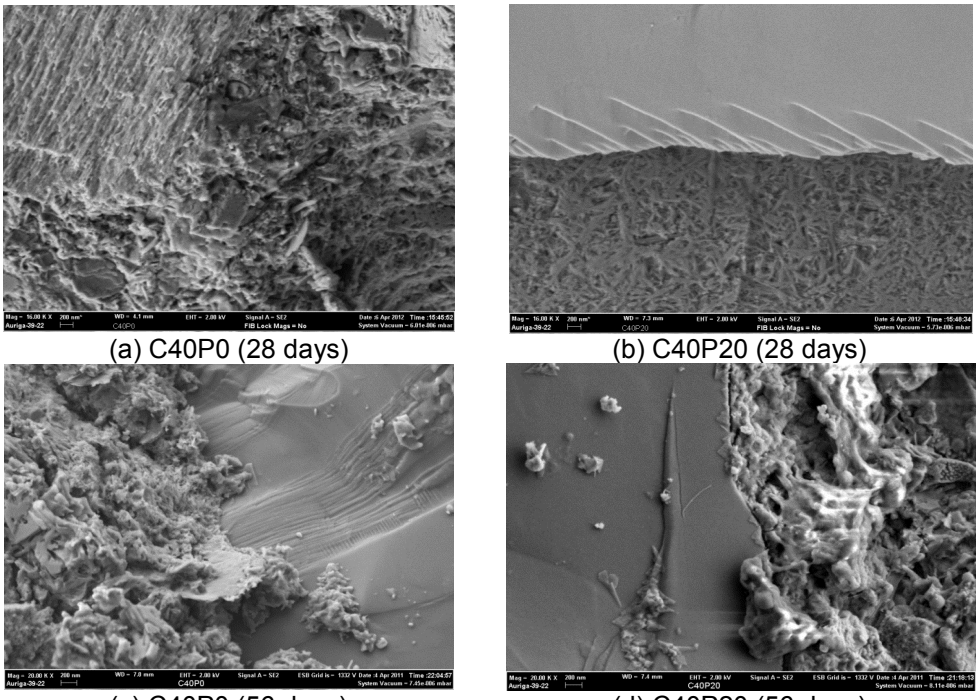

(a) C40P0 (28 days) (b) C40P20 (28 days)

(c) C40P0 (56 days) (d) C40P20 (56 days)

Fig. 7. Effect of POFA on the microstructure of concrete (W/B = 0.40; 28 and 56 days)

4. CONCLUSIONS

The following conclusions are drawn based on the findings of the present study regarding the microstructure of SCHSC incorporating POFA.

1. POFA produced a significant effect on the microstructure of SCHSC. The SEM images of the concretes revealed that POFA contributed to produce a denser microstructure due to its microfilling ability and pozzolanic activity. The improvement of concrete microstructure occurred in both bulk paste matrix and interfacial transition zone with a reduced porosity.

2. The amount of porous hexagonal $Ca(OH)_2$ crystals was significantly reduced at the early ages of SCHSC including POFA. There observed minimum $Ca(OH)_2$ crystals at the later ages of SCHSC with POFA. As a result, the SCHSC with POFA became less porous than the SCHSC without POFA.

3. The predominant product phase at the later ages was C-S-H for all SCHSCs. There was no needle-like ettringite product in the SEM of the later-age concretes. Some $Ca(OH)_2$ crystals were observed in the SEMs of the SCHSCs without POFA; these crystals were significantly reduced in all SCHSCs including POFA. This is because the $Ca(OH)_2$ crystals were consumed when reacted with the silica (SiO_2) content of POFA during pozzolanic reaction.

4. The porosity and width of interfacial transition zone were substantially reduced in SCHSC including POFA. This is also attributed to the microfilling ability and pozzolanic activity of POFA. In particular, the secondary hydration products resulting from the pozzolanic reaction significantly contributed to reduce the porosity and width of transition zone.

5. The highest compressive strength and the lowest permeable porosity were achieved for the SCHSCs incorporating 20% POFA. These results were consistent with the microstructural observations in SCHSCs with 20% POFA.

ACKNOWLEDGEMENTS

The authors gratefully acknowledge the financial support from the University of Malaya, Kuala Lumpur, Malaysia (research grant: UMRG RP018/2012A). The authors are also thankful to Jugra Palm Oil Mill Sdn. Bhd., Banting, Selangor Darul Ehsan, Malaysia for supplying palm oil fuel ash for this research.

COMPETING INTERESTS

Authors have declared that no competing interests exist.

REFERENCES

1. Ganesan K, Rajagopal K, Thangavel K. Evaluation of bagasse ash as supplementary cementitious material. Cement and Concrete Composites. 2007;29(6):515–524.
2. Zhang MH, Lastra R, Malhotra VM. Rice-husk ash paste and concrete: Some aspects of hydration and the microstructure of the interfacial zone between the aggregate and paste. Cement and Concrete Research. 1996;26(6):963–977.
3. Safiuddin Md. Development of self-consolidating high performance concrete incorporating rice husk ash. Ph.D. Thesis. Waterloo, Ontario, Canada: University of Waterloo; 2008.
4. Xie Y, Liu B, Yin J, Zhou S. Optimum mix parameters of high-strength self-compacting concrete with ultrapulverized fly ash. Cement and Concrete Research. 2002;32(3):477–480.
5. Sumadi SR, Hussin MW. Palm oil fuel ash (POFA) as a future partial cement replacement material in housing construction. Journal of Ferrocement. 1995;25:25–34.
6. Tonnayopas D, Nilrat F, Putto K, Tantiwitayawanich J. Effect of oil palm fiber fuel ash on compressive strength of hardening concrete. In: Proceedings of the 4th Thailand Materials Science and Engineering; 2006; Thailand: Pathumthani. 2006;1–3.
7. Safiuddin Md, Salam MA, Jumaat MZ. Utilization of palm oil fuel ash in concrete: a review. Journal of Civil Engineering and Management. 2011;17(2):234–247.
8. Tay J-H, Show K-Y. Use of ash derived from oil-palm waste incineration as a cement replacement material. Resources, Conservation and Recycling. 1995;13(1):27–36.
9. Tangchirapat W, Saeting T, Jaturapitakkul C, Kiattikomol K, Siripanichgorn A. Use of waste ash from palm oil industry in concrete. Waste Management. 2007;27(1):81–88.
10. James J, Rao MS. Reaction product of lime and silica from rice husk ash. Cement and Concrete Research. 1986;16(1):67–73.
11. Gao JM, Qian CX, Liu HF, Wang B, Li L. ITZ microstructure of concrete containing GGBS. Cement and Concrete Research. 2005;35(7):1299–1304.
12. Tuan NV, Ye G, Breugel KV, Copuroglu O. Hydration and microstructure of ultra high performance concrete incorporating rice husk ash. Cement and Concrete Research. 2011;41(11):1104–1111.
13. Altwair NM, Johari MAM, Hashim SFS. Strength activity index and microstructural characteristics of treated palm oil fuel ash. International Journal of Civil and Environmental Engineering. 2011;11(5):100–107.
14. Eldagal OEA. Study on the behaviour of high-strength palm oil fuel ash (POFA) concrete. M.Sc. Engg. Thesis. Skudai, Malaysia: Universiti Technologi Malaysia; 2008.
15. ASTM C 136-06. Standard test method for sieve analysis of fine and coarse aggregates. Annual Book of ASTM Standards, vol. 04.02. Philadelphia, USA: American Society for Testing and Materials (ASTM); 2006.
16. ACI 211.4R-08. Guide for selecting proportions for high-strength concrete using portland cement and other cementitious materials. ACI Manual of Concrete Practice, Part 1. Farmington Hills, Michigan, USA: American Concrete Institute (ACI); 2008.
17. ASTM C 1611/C 1611M-09a. Standard test method for slump flow of self-consolidating concrete. Annual Book of ASTM Standards, vol. 04.02. Philadelphia, USA: American Society for Testing and Materials (ASTM); 2009.
18. ASTM C 39/C 39M. Standard test method for compressive strength of cylindrical concrete specimens. Annual Book of ASTM Standards, vol. 04.02. Philadelphia, USA: American Society for Testing and Materials (ASTM); 2009.
19. ASTM C 642. Standard test method for density, absorption, and voids in hardened concrete. Annual Book of ASTM Standards, vol. 04.02. Philadelphia, USA: American Society for Testing and Materials (ASTM); 2009.

20. EFNARC. Specifications and guidelines for self-consolidating concrete. Surrey, UK: The European Federation of Suppliers of Specialist Construction Chemicals (EFNARC); 2002.
21. Safiuddin Md, Alengaram UJ, Salam MA, Jumaat MZ, Jaafar FF, Saad HB. Properties of high-workability concrete with recycled concrete aggregate. Materials Research. 2011;14(2):1–8.
22. ASTM C 618-08a. Standard specification for fly ash and raw or calcined natural pozzolan for use as a mineral admixture in portland cement concrete. Annual Book of ASTM Standards, vol. 04.02. Philadelphia, USA: American Socity for Testing and Materials (ASTM); 2008.
23. Awal ASMA. A study of strength and durability performances of concrete containing palm oil fuel ash. Ph.D. Thesis. Skudai, Malaysia: Universiti Teknologi Malaysia; 1998.
24. Hearn N, Hooton RD, Mills RH. In: Significance of tests and properties of concrete and concrete-making materials: pore structure and permeability. Philadelphia, USA: American Society for Testing and Materials (ASTM). 1994;240–262.

Peer-review history:
The peer review history for this paper can be accessed here:
http://www.sciencedomain.org/review-history.php?iid=224&id=4&aid=1814